JOC The Journal of Organic Chemistry

Article

pubs.acs.org/joc

Photochromic C2-Symmetric Chiral Diarylethene: From the Initial State to the Final State

Stéphanie Delbaere,*[,†] Jérôme Berthet,[†] Tatsuya Shiozawa,[‡] and Yasushi Yokoyama*[,‡]

[†]University Lille Nord de France, CNRS UMR 8516, UDSL, Lille, F-59006 Lille Cedex, France

[‡]Department of Advanced Materials Chemistry, Yokohama National University, Tokiwadai, Hodogaya, Yokohama 240-8501, Japan

Supporting Information

ABSTRACT: The behavior of 1,2-bis[(*R*)-2-(1-methoxymethoxyethyl)-3-benzo[*b*]-thienyl] hexafluorocyclopentene before and upon UV irradiation and during thermal evolution of the photoirradiated solution has been thoroughly investigated by multinuclear NMR spectroscopy. A dynamic NMR study of the initial state was performed, providing a detailed description of the perceived conformational processes in the system. Before irradiation, three open conformations are in equilibrium, whereas UV irradiation generated the two expected cyclized diastereomers. The minor diastereomer was thermally less stable than the major one, thus leading to an unexpected increase in the diastereoselectivity when raising the photoirradiation temperature. In addition, a long thermal evolution induced slow rearrangement of the stable diastereomer into byproducts that were identified.

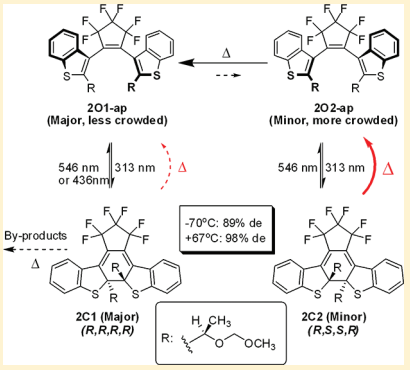

INTRODUCTION

Organic photochromic compounds[1−4] allowing reversible modulation of physical properties upon an external trigger are very promising for applications in optoelectronics devices or high-density optical memories.[5−9] Diarylethenes are one of the most promising photochromic compounds for the applications because of their excellent fatigue resistance and their thermal irreversibility.[10,11] Their photochromism is based on the conrotatory 6π-electrocyclization between a hexatriene and a cyclohexadiene, generating a pair of enantiomers from the photoreactive antiparallel conformers.[12] Usually, generation of enantiomers does not cause any problems. However, when the photochromism is applied to the biological systems or chiral materials such as cholesteric liquid crystals, formation of enantiomers may make the system complicated or one of the enantiomers could be harmful or could compensate the properties brought about by the photochromic reactions. When the molecule possesses at least one chiral center, the photochromic ring closure produces a pair of diastereomers instead of enantiomers.[13] If the chiral centers are located close to the hexatriene moiety and control the helical conformation of the hexatriene moiety effectively, then only one diastereomer of the cyclohexadiene isomer may be generated upon the photochromic ring closure. The Japanese members of the authors have been engaged in developing an effective and universal protocol to realize highly diastereoselective photochromic reactions of diarylethenes. Recently, one of us reported the exceptionally high diastereoselectivity in the photochemical ring closure of bisbenzothienylethenes **1** and **2** (Scheme 1) having two (*R*)-methoxymethoxyethyl groups that act as the controller of the helical conformation of the hexatriene.[14]

Scheme 1. Structures of 1,2-Bis[(*R*)-3-(1-methoxymethoxyethyl)-2-benzo[*b*]thienyl]hexafluorocyclopentene 1O and 1,2-Bis[(*R*)-2-(1-methoxymethoxyethyl)-3-benzo[*b*]thienyl]hexafluorocyclopentene 2O

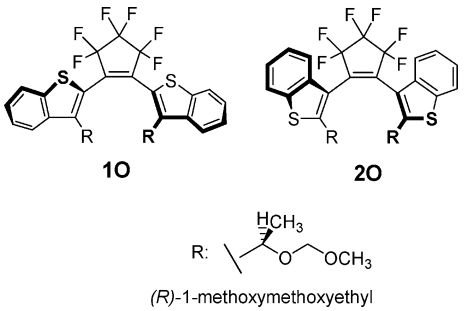

One way to alter the population of the diastereomeric conformers is to change the temperature of the solution. It is well-known that when the temperature is lowered, the Boltzmann distribution of the conformational isomers at the ground state shifts to the more stable one. While compound **1O**, whose bisbenzothienyl groups are connected to perfluorocyclopentene with their C-2 atoms showed the expected increase of the diastereoselectivity by lowering the photoirradiation temperature, compound **2O** whose bisbenzothienyl groups are connected to perfluorocyclopentene at C-3 did not behave as expected. Moreover, when the irradiation temperature was raised, the diastereoselectivity increased. To elucidate how this strange phenomenon happened, which is against the common

Received: November 30, 2011
Published: January 25, 2012

dx.doi.org/10.1021/jo202466g | *J. Org. Chem.* 2012, 77, 1853−1859

sense of chemists, and because temperature-dependent studies make it possible to reveal new aspects and limits of the switching processes,[15−17] we undertook an intensive structural investigation by NMR spectroscopy of **2O** before, during and after irradiation. During the research, first the thermodynamic behavior of the initial state was fully examined, with a dynamic NMR study, which provided detailed description of perceived conformational processes in the system.[18−24] Then, the complete structural analysis of the final state was carried out. Several minor byproducts generated either photochemically or thermally were found. Although they were detected only by NMR, the structures were fully characterized.

RESULTS AND DISCUSSION

Investigation of 1O. For the sake of comparison, the photochemical behavior of **1O** in toluene at room temperature was first investigated before and after irradiation with 313 nm light. It is known that both antiparallel and parallel conformations cannot be separated by NMR due to the fast interconversion between them.[25,26] Then, only one set of signals was observed for the open form (Figure 1a), and the

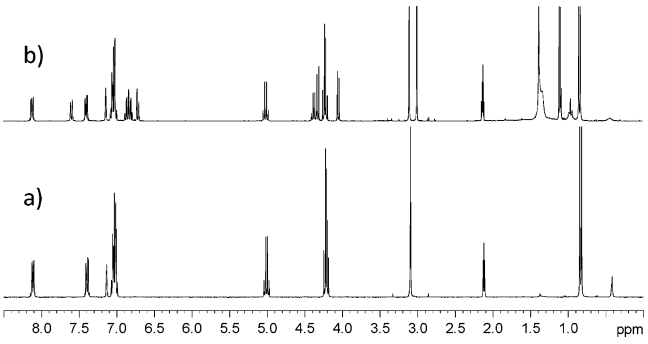

Figure 1. ^{1}H NMR spectra of **1O** (a) before and (b) after irradiation with 313 nm light at rt in toluene.

irradiation with UV light resulted in the detection of only one cyclized diastereomer **1C** (Figure 1b).

Investigation of 2O before Irradiation. To the contrary, in the ^{1}H 500 MHz NMR spectrum of **2O** in toluene-d_8 at room temperature, four separate doublets of the secondary methyl group of the conformational isomers (δ 0.31, 1.48, 1.22, and 1.72, in the ratio 88:9:1.5:1.5) are observed (Figure 2).

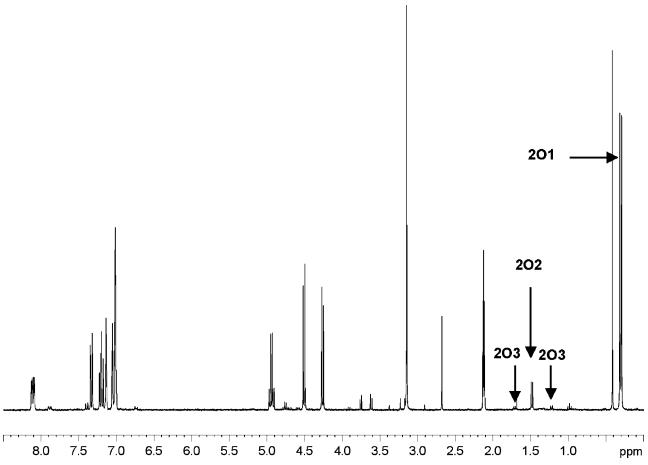

Figure 2. ^{1}H NMR spectrum of **2O** at rt in toluene.

These are associated with three conformations; two are symmetrical [**2O1** (88%), **2O2** (9%)], and the third is dissymmetrical [**2O3** (3%)].

Variable-temperature NMR did not underline any coalescence of signals in the range from −80 up to +100 °C. Instead, a variation in the ratio between the conformers was observed. More particularly, the distribution between the two symmetrical conformers is more affected between −10 °C and +75 °C. Outside of this range, the ratio remains almost unchanged, being at about 94:6 below −10 °C and reaching 87:13 at T > 75 °C. On the other hand, the ratio of the third conformer did not greatly change, being less than 1% at −80 °C, reaching 3% at rt, and being no longer detected at T > 63 °C due to a large broadening of its signals. In each spectrum recorded at each temperature, no evolution in concentration is obtained, indicating that the three conformers are in total equilibrium. Then, the ratio of their concentrations gives access to the equilibrium constant K_{eq}. Consequently, the equilibrium constants K_{eq1-3} = **2O1**/**2O3** = k_{31}/k_{13}, K_{eq3-2} = **2O3**/**2O2** = k_{23}/k_{32}, K_{eq1-2} = **2O1**/**2O2** = k_{21}/k_{12}, were calculated, and their natural logarithm values were plotted as a function of $1/T$. Straight lines following the van't Hoff law were obtained (Figure 3), from which the thermodynamic parameters were deduced.

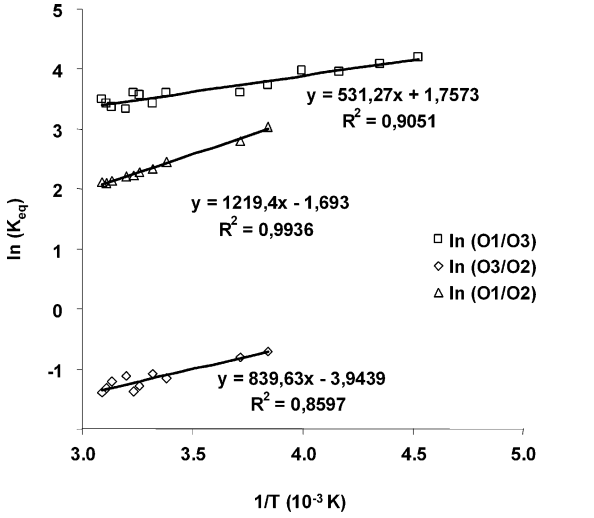

Figure 3. van't Hoff plot.

Indeed, as the Gibbs standard free energy change $\Delta G^\circ = -RT \ln K_{eq}$ is related to $\Delta H^\circ - T\Delta S^\circ$, the slope and the intercept of $\ln K_{eq} = f(1/T)$ enabled the estimation of ΔH° and ΔS° for each process (Figure 4).

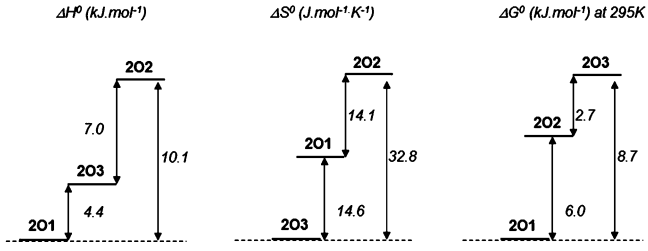

Figure 4. Enthalpy and entropy variation diagram and resulted Gibbs standard free energy change at 295 K.

The Gibbs free energy difference ΔG° between **2O1** and **2O3** and between **2O3** and **2O2** corresponds to the calculated

dx.doi.org/10.1021/jo202466g | J. Org. Chem. 2012, 77, 1853−1859

$\Delta G°$ between **2O1** and **2O2**, whereas those relationships for enthalpy and entropy values show some discrepancy. However, the thermodynamic parameters are directly extracted from the slope and the intercept of the corresponding straight lines, the coefficients R^2 of which are not equal but very close to 1. The small observed deviations can result from peak integrations in NMR spectra, particularly for data measured for **2O3**, which is the lowest concentrated compound in solution. Nevertheless, the thermodynamic parameters can be agreed as the significance levels are all higher than 99% (see Supporting Information). Examination of enthalpy difference indicates that the order of stability of the conformers is **2O1** > **2O3** > **2O2** (Figure 4 left), whereas entropy differences give the order of **2O2** > **2O1** > **2O3** (Figure 4, middle). The entropy term indicates that **2O3** has the least freedom (probably suffering large steric restriction between the side chains) of the molecular motion and **2O2** has the largest freedom, despite the consideration that it must be sterically more congested than **2O1**. The stability of the system is expressed by ΔG. When ΔG is positive, the system is less stable, and when ΔG is negative, the system is more stable. Thus, the stability in terms of ΔG is increased when associated with a small ΔH value or with a large ΔS contribution. **2O1** presents the smallest enthalpy value; it is the most stable in terms of ΔH. **2O2** has the largest entropy value and contributes to increase in the stability of the system ($\Delta G°$). Therefore, from the entropy viewpoint, the contribution of ΔS is the largest for **2O2** and the smallest for **2O3**. The order in which the contribution of ΔS is the largest is **2O2**, the smallest is **2O3**. However, the order of stability indicated by the Gibbs free energy difference $\Delta G°$ is reasonable, as **2O1** > **2O2** > **2O3** (Figure 4 right) in a perfect agreement with the ratio measured in NMR spectra. Irie reported that the calculated $\Delta G°$ of antiparallel and parallel conformers of **2O** (R = *i*Pr) by AM1 semiempirical MO theory is about 4 kJ mol^{-1}, whereas the NMR data described in the text (the population of two conformers is 94/6) gave the value of 6.8 kJ mol^{-1}.[27] The latter, obtained from the experiments, is in fairly good accordance with the $\Delta G°$ difference between **2O1** and **2O3**, 8.7 kJ mol^{-1}.

To complete this thermodynamic study, 2D-EXSY experiments giving the information on the site-exchange rates were performed with different mixing times at rt, as the concentration and spectral resolution of **2O3** is the best at this temperature. From off-diagonal exchange cross-peaks originating from different species, the exchange rate constants $k_{exsy} = k_{13} + k_{31}$ and $k_{23} + k_{32}$ were extracted by plotting intensity = f(mixing time)[28] (see Supporting Information for details). As $k_{exsy} = k_{13} + k_{31}$ and $k_{23} + k_{32}$, using the previous equilibrium constant measured at rt, it is possible to determine the values of k_{13}, k_{31}, k_{23}, and k_{32} (Scheme 2). These rates are relatively slow so that we were able to observe the site exchange in EXSY. Finally, calculation of $\Delta G^{‡}$ with each k value of back and forth site changes using Eyring equation ($\Delta G^{‡} = -RT \ln (kh/\kappa k_B T)$, assuming a transmission coefficient $\kappa = 1$) at T = 295 K results in $\Delta G_{13}{}^{‡}$ = 83.54 kJ mol^{-1}, $\Delta G_{31}{}^{‡}$ = 74.68 kJ mol^{-1}, $\Delta G_{23}{}^{‡}$ = 78.49 kJ mol^{-1}, and $\Delta G_{32}{}^{‡}$ = 75.65 kJ mol^{-1}. Differences of each exchange reaction are 8.86 kJ mol^{-1} and 2.84 kJ mol^{-1}, respectively, which is in good accordance with $\Delta G°$ values shown in Figure 4 (8.7 and 2.7 kJ mol^{-1}).

By combining these results with ^{1}H, ^{13}C, and ^{19}F NMR data, the conformations drawn in Scheme 2 can be proposed. The two C2-symmetric antiparallel conformers (2O1 and 2O2) are assigned to the less crowded and more stable one and to the more crowded and more unstable one, respectively. When the

Scheme 2. Equilibrium between the Three Conformers of 2O

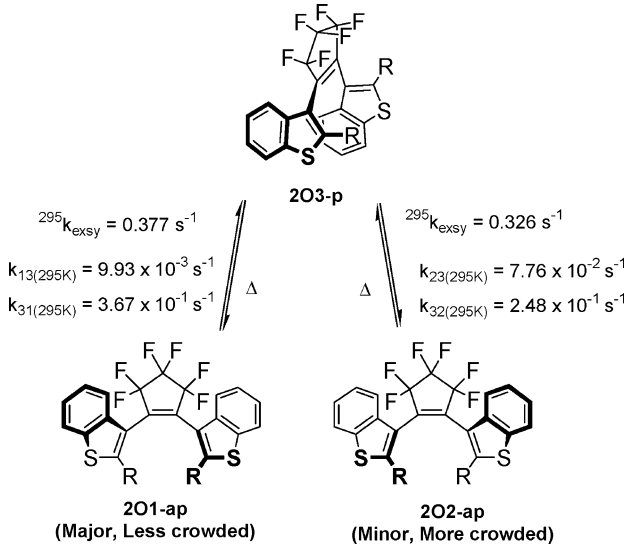

temperature is lowered, the Boltzmann distribution of the conformational isomers at the ground state shifts to the more stable one, and therefore when the temperature is raised, the population of the minor conformer increases. As for the dissymmetric **2O3**, it is the parallel conformer that cannot cyclize due to the restriction of Woodward−Hoffmann rules. It plays an intermediate role in the conformation change between the two antiparallel conformers, **2O1** and **2O2**.

Photochromism of 2O upon UV Irradiation. Photochemical ring closure of **2O** was conducted in toluene at −60 °C, at rt (Figure 5), and at +80 °C with 313 nm light.

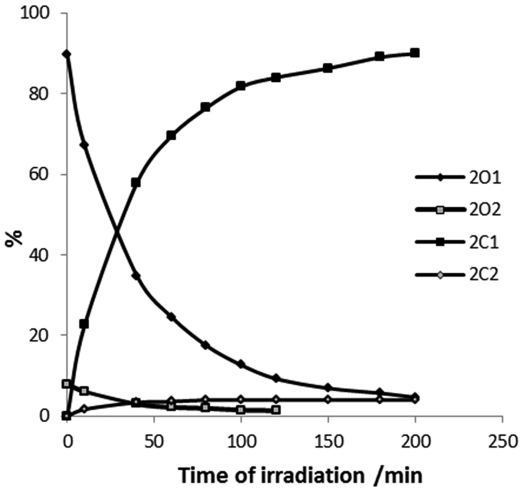

Figure 5. Time evolution of **2O** upon irradiation with 313 nm light at rt in toluene.

Two diastereomers **2C1** and **2C2** were formed at low and room temperatures, as indicated by the decrease of signal intensity of methoxy groups in **2O1** (δ 3.15 ppm) and **2O2** (δ 2.67 ppm) and the appearance of new resonances at 3.00 (**2C1**) and 2.97 (**2C2**) ppm (Figure 6). Upon irradiation with 536 nm light, the two cyclized diastereomers returned toward the initial mixture of **2O1** + **2O2**. Such observations are in complete agreement with the expected behaviors. The

dx.doi.org/10.1021/jo202466g | J. Org. Chem. 2012, 77, 1853−1859

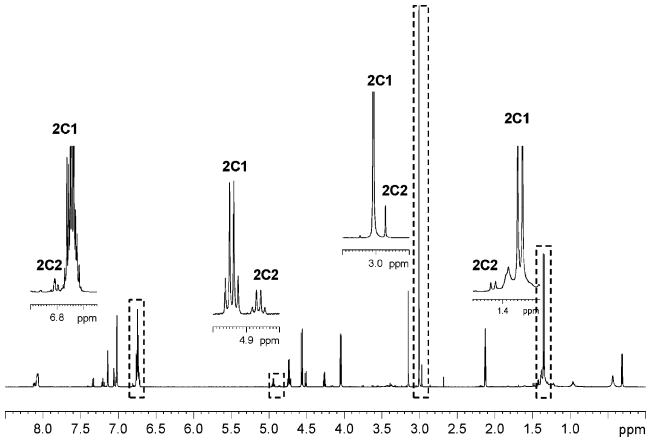

Figure 6. ^{1}H NMR spectrum of **2O** after irradiation at −60 °C in toluene.

photogenerated closed-ring form **2C** has an asymmetric structure with either *SS* or *RR* stereochemistry, and the stereochemistry on the side chain is *R*. Consequently, the two diastereomers *R*-(*RR*)-*R* and *R*-(*SS*)-*R* can be distinguished by NMR. At −60 °C, the ratio between both antiparallel conformations of **2O** is 94:6 and irradiation generates a ratio of 94:6, whereas at rt, irradiation of a 91:9 mixture produces a ratio of 96:4 of cyclized forms. Thus, similarly to the previous report,[14] the same unexpected de values (88% at low temperature and 92% at rt) are observed. No byproducts are observed at the end of the irradiation period. In contrast, when irradiation was applied at +80 °C, only the cyclized structure **2C1** was produced and new resonances assigned to another compound **2C3** were detected, whereas no **2C2** was observed. At this temperature, the aromatized compound with elimination of aliphatic chains,[25,26,29−31] **D1**, and methyl formate, **D2**, have also been detected. Finally, it must be noted that the ratio between **2O1** and **2O2** remained stable at 87:13.

Thermal Evolution of 2C1 + 2C2. An irradiated solution of **2O**, constituted by a mixture of **2C1** + **2C2** was kept in the dark at 295 K over a period of several weeks, and its thermal evolution at 295 K was followed by NMR. It turned out that **2C2** returned to the initial **2O2** (k = 0.28 day^{-1}), whereas **2C1** evolved toward the structure **2C3** (k = 0.023 day^{-1}). The thermal instability of **2C2** and the appearance of **2C3** are in agreement with experiment performed at +80 °C, where **2C2** was not detected and **2C3** was observed, indicating the occurrence of thermal reactions. To accelerate the thermal conversion of **2C1** into **2C3**, the sample was heated at 60 °C for 12 h. To our surprise, the formation of a new compound, **2C4**, was evidenced.

Photobleaching of the Mixture of 2C1 + 2C3 with Visible Light. Irradiation with 546 nm light was applied to a sample containing **2C1** + **2C3**. The opening of the cyclized **2C1** is very efficient, whereas **2C3** is not reactive. Irradiation with 436 nm light of another sample bleached both **2C1** and **2C3** with the bleaching rate of **2C3** twice as fast as that of **2C1**. However, while **2C1** returns fully toward the initial **2O1** form, **2C3** is converted to several new byproducts, which could not be identified due to their large number of resonances associated with the absence of coupling. This result indicates that **2C3** has absorption at 436 nm but does not absorb at 546 nm. The set of observed reactions is summarized in Table 1.

Structural Elucidation of Photoproducts of 2O. An extensive structural identification was conducted by carrying out a set of 1D and 2D multinuclear (^{1}H, ^{13}C, and ^{19}F) NMR experiments. First, examining **2C1**, the cyclization is proved by ^{1}H−^{13}C 2D-HMBC with long-range couplings observed between H at 4.73 ppm and quaternary carbons at 144.4 and 69.7 ppm. The latter is also scalar coupled with CH_3 at 1.35 ppm. Dipolar correlations are observed between an aromatic proton at 8.07 ppm with the MOM aliphatic chain, and the strongest effect with the secondary methyl group at 1.35 ppm. In addition, 2D-HOESY evidence shows dipolar correlations between fluorines Fa = Fc at −108 ppm and Fa′ = Fc′ at −117.5 ppm with H at 4.73 ppm. The ^{1}H spectrum of **2C2** is very similar to that of **2C1**, although the amount produced is much less, and it was revealed that **2C2** is thermally unstable and goes back to **2O2**. Consequently, **2C1** and **2C2** are generated from **2O1** and **2O2** respectively, and are attributed to the *R*-(*RR*)-*R* and *R*-(*SS*)-*R* diastereomers.

In order to elucidate the reason why **2C2** is thermally unstable, DFT calculations were carried out. However, due to the vast freedom of the rotation of the methoxymethoxyethyl (MOMO) moiety, it was not possible to obtain the most stable conformation. In the ^{1}H−^{19}F HOESY spectrum (Figure 7), strong interactions between the hydrogen on the chiral carbon atom and the fluorine atoms Fa = Fc and Fa′ = Fc′ were observed, while no interaction was shown between the fluorine atoms and the methyl group on the chiral carbon atom or the protons on the MOMO group.

This means that the structure around the C−C bond connecting the main ring structure and the chiral substituent is as shown in Figure 8a. In this structure, the MOMO group is located in a sterically less hindered region. To the contrary, if the MOMO group of **2C2** is located in the same region (Figure 8b), the

Table 1. Summary of Observed Reactions; Initial State Concerns Compounds that React upon the Described Experimental Conditions

initial state	experimental conditions	final state
2O1 + **2O2**	313 nm, −60 °C	**2C1** (87%) + **2C2** (6%) at PSS
2O1 + **2O2**	313 nm, rt	**2C1** (90%) + **2C2** (4%) at PSS
2O1 + **2O2**	313 nm, +80 °C, 10 min	**2C1** (27%) + **2C3** (11%)
	313 nm, +80 °C, 20 min	**2C1** (28%) + **2C3** (20%) + **D1**-**D2** (20%)
2C1 + **2C2**[a]	546 nm	**2O1** + **2O2**
2C1 + **2C2**[a]	Δ (295 K)	**2C3** (slow) + **2O2** (fast)
2C3[a]	Δ (333 K)	**2C4**
2C1 + **2C3**[a]	546 nm	**2O1** + **2C3**
2C1 + **2C3**[a]	436 nm	**2O1** + byproduct

[a]Solutions that are mixtures of cyclized compounds with open conformers **2O**.

dx.doi.org/10.1021/jo202466g | J. Org. Chem. 2012, 77, 1853−1859

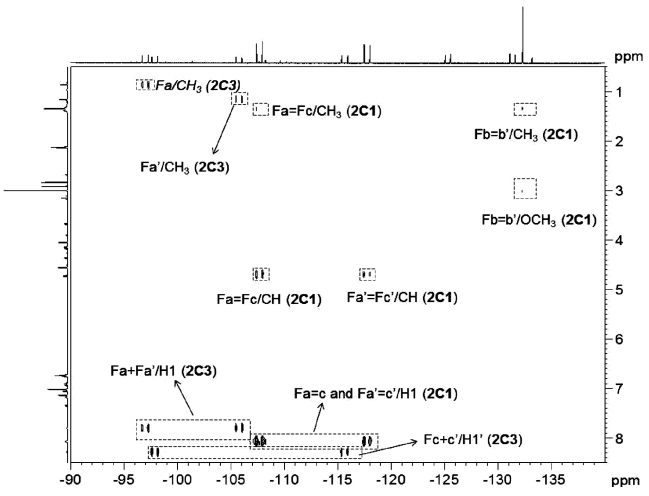

Figure 7. $^{1}H-^{19}F$ HOESY NMR spectrum.

secondary methyl group will replace the space where the hydrogen is located in **2C1**. In this rotamer, the distance between the secondary methyl group and the fluorine atoms is so small that there must be a strong steric repulsion. If the hydrogen atom on the asymmetric carbon atom of **2C2** is located in the same space as in **2C1** (Figure 8c), then the MOMO group will come above the cyclohexadiene moiety so that it would become sterically much more unstable. Therefore the structure of **2C2** itself includes the steric instability so that much faster thermal back reaction of **2C2** compared to that of **2C1** occurred.

Concerning the thermally generated compound **2C3**, its structure is dissymmetric. 1D and 2D NMR experiments were applied to achieve its structural identification (Figure 9). HMBC underlines long-range couplings between H at 3.9 ppm and quaternary carbons at 146.8 and 70.2 ppm, between H at 4.14 ppm and quaternary carbons at 65 and 137.2 ppm, between CH_3 at 1.15 ppm and aliphatic quaternary carbon at 70.2, and between CH_3 at 0.86 ppm and aliphatic quaternary carbon at 65 ppm.

Dipolar contacts are also measured between CH_3 at 0.86 ppm and an aromatic proton at 7.79 ppm and with fluorine Fa at −96.8 ppm, while the CH_3 at 1.15 ppm is spatially close to Fa′ at −105.7 ppm (Figure 7). **2C3** being structurally identified, its formation could be explained from a thermal [1,5]-sigmatropic reaction that involves the retention of absolute stereochemistry of the asymmetric carbon atom on the rearranging group, according to the Woodward−Hoffmann rules for thermal sigmatropic reactions. Namely, one of the side chains is transferred from the ring-forming carbon atom to the carbon atom next to the perfluorocyclopentene ring on the

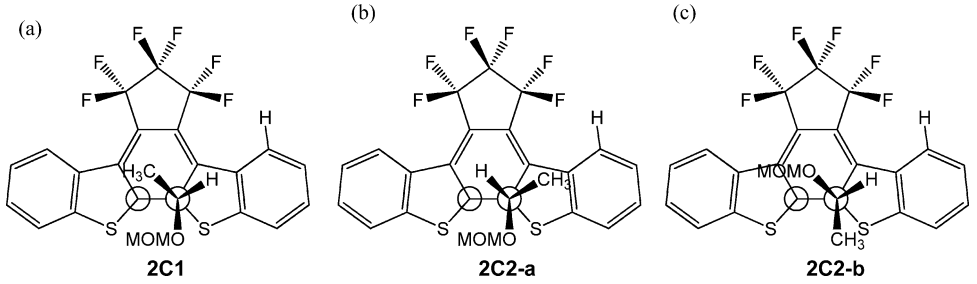

Figure 8. Rotamers of C-forms. (a) **2C1** predicted by 2D HOESY experiment, (b, c) possible rotamers of **2C2**. The chiral substituent on the left side is not depicted for clarity.

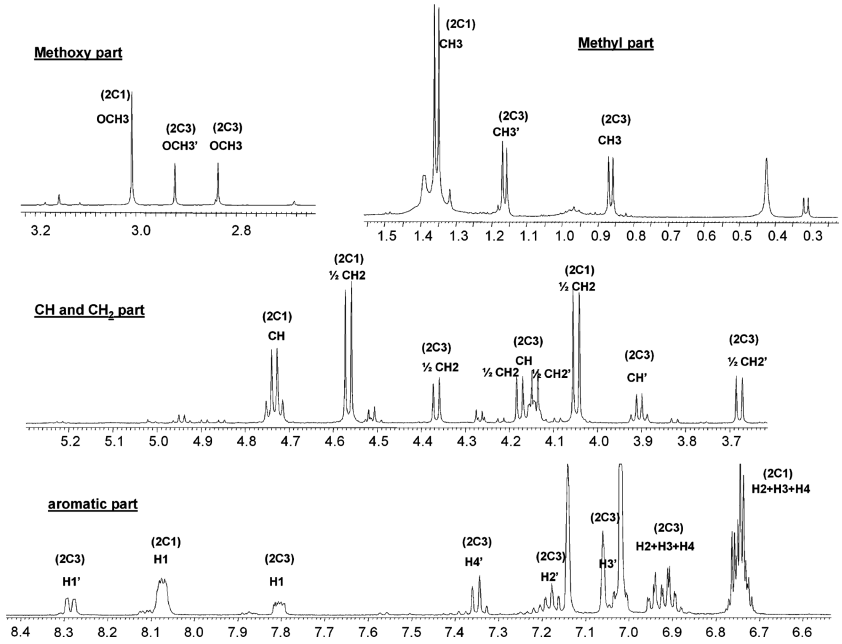

Figure 9. ^{1}H NMR spectrum with assignments of protons in **2C1** and **2C3**.

dx.doi.org/10.1021/jo202466g | J. Org. Chem. 2012, 77, 1853−1859

Scheme 3. Photochromic Reaction of (*R*,*R*)-1,2-Bis[2-(1-methoxymethoxyethyl)-3-benzo[*b*]thienyl]-hexafluorocyclopentene

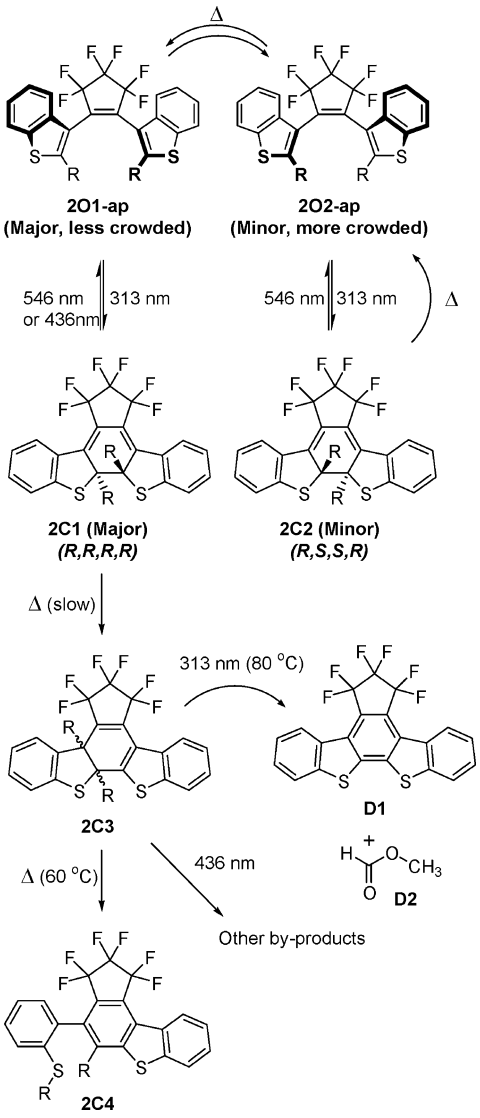

other thiophene. There the side chain is so close to the phenyl proton that there are strong NOE signals.

2C4 was fully characterized by a set of NMR experiments, and it corresponds to the byproduct recently reported by Kobatake.[32] One of the aliphatic side chains was transferred to the sulfur atom of one thienyl ring in close proximity concomitant with the ring cleavage. This rearrangement generates a phenyl ring at the center of the molecule.

CONCLUSION

The behavior of the bisbenzothienylethene **2O** having two (*R*)-methoxymethoxyethyl groups that control the helical conformations in solution at various temperatures has been investigated. The equilibrium between three open conformations, two antiparallel and one parallel, has been quantified with the determination of the thermodynamics parameters. Photoirradiation at low, room, and high temperatures was applied and revealed that the two expected diastereomeric cyclized compounds are produced. The uncommon decrease of diastereoselectivity by lowering the photoirradiation temperature was explained as the result of the lower thermal stability of the minor diastereomer. In contrast, over a very long period of thermal evolution in the dark, the more stable diastereomer slowly evolved toward byproducts that were detected and identified, as the result of unexpected rearrangements. The whole reaction scheme of the photochromic compound was clarified and is summarized in Scheme 3.

EXPERIMENTAL SECTION

Irradiation Device. Photoirradiation was carried out directly in the NMR tube in a home-built apparatus. The emission spectrum of a 1000 W Xe–Hg high-pressure short-arc lamp, filtered by a band-pass glass filter then through an interferential one (UV 259 < λ < 388 nm with λ_{max} =330 nm, T = 79%, and λ = 313 nm and T = 16%; visible 295 < λ < 800 nm with T = 50% at λ = 330 and 700 nm, and λ = 436 nm and T = 50% or λ = 546 nm and T = 62%) was focused on the end of a silica light-pipe (length 6 cm, diameter 8 mm), leading the light to the spinning sample tube, which was inserted in a quartz dewar. The temperature of the sample was controlled with a variable temperature unit. After irradiation, the NMR sample tube was rapidly transferred to the NMR probe, which is thermoregulated at the same temperature as that used within irradiation. Photoirradiation was applied at regulated temperature (−60 °C, rt, and +80 °C).

NMR Experiments. NMR spectra of samples in CD_3CN (5.10^{-3} M) were recorded on a 500 spectrometer (^1H, 500 MHz; ^{13}C, 125 MHz; ^{19}F, 470 MHz) equipped with TXI or QNP probe, using standard sequences. Data sets were processed using Topspin 2.1 software.

ASSOCIATED CONTENT

Supporting Information

Details of irradiation techniques, NMR experiments. This material is available free of charge via the Internet at http://pubs.acs.org.

AUTHOR INFORMATION

Corresponding Author

*E-mail: stephanie.delbaere@univ-lille2.fr; yyokoyam@ynu.ac.jp.

ACKNOWLEDGMENTS

The 500 MHz NMR facilities were funded by the Région Nord-Pas de Calais (France), the Ministère de la Jeunesse, de l'Education Nationale et de la Recherche (MJENR) and the Fonds Européens de Développement Régional (FEDER). Part of this collaborative work was realized within the framework GDRI CNRS 93 "Phenics" (Photoswitchable Organic Molecular Systems & Devices). Preparation of compounds was aided by a Grant-in-Aid text.

REFERENCES

(1) *Photochromism: Molecules and Systems*; Dürr, H., Bouas-Laurent, H., Eds.; Elsevier: Amsterdam, 1990.
(2) *Organic Photochromic and Thermochromic Compounds*; Crano, J. C., Guglielmetti, R. J., Eds.; Plenum Press: New York, 1999.
(3) *Molecular Switches*; Feringa, B. L., Ed.; Wiley-VCH: New York, 2001.
(4) *Photo-Reactive Materials for Ultrahigh-Density Optical Memory*; Irie, M., Ed.; Elsevier: Amsterdam, 1994.
(5) Browne, W. R.; Feringa, B. L. *Nat. Nanotechnol.* **2006**, *1*, 25–35.
(6) Latini, G.; Parrott, L.-J.; Brovelli, S.; Frampton, M. J.; Anderson, H. L.; Cacialli, F. *Adv. Funct. Mater.* **2008**, *18*, 2419–242.
(7) Strassert, C.; Otter, M.; Albuquerque, R. O.; Höne, A.; Vida, Y.; Maier, B.; De Cola, L. *Angew. Chem., Int. Ed.* **2009**, *48*, 7928–7931.
(8) *Smart Materials In Architecture, Interior Architecture and Desig*; Ritter, A., Ed.; Birkhäuser: Basel, 2007.

(9) Balzani, V.; Bergamini, G.; Ceroni, P. *Coord. Chem. Rev.* **2008**, *252*, 2456−2469.
(10) (a) Irie, M.; Uchida, K. *Bull. Chem. Soc. Jpn.* **1988**, *71*, 985−996. (b) Irie, M.; Mohri, M. *J. Org. Chem.* **1988**, *53*, 803−808.
(11) Irie, M. *Chem. Rev.* **2000**, *100*, 1685−1716.
(12) Yokoyama, Y. *New J. Chem.* **2009**, *33*, 1314−1319.
(13) Tani, Y.; Ubukata, T.; Yokoyama, Y.; Yokohama, Y. *J. Org. Chem.* **2006**, *72*, 1639−1644.
(14) Yokoyama, Y.; Shiozawa, T.; Tani, Y.; Ubukata, T. *Angew. Chem., Int. Ed.* **2009**, *48*, 4521−4523.
(15) Irie, M.; Eriguchi, T; Takada, T.; Uchida, T. *Tetrahedron* **1997**, *53*, 12263−12271.
(16) Kuldova, K.; Tsyganenko, K.; Corval, A.; Trommsdorff, H. P.; Bens, A. T.; Kryschi, C. *Synth. Met.* **2000**, *115*, 163−166.
(17) Dulic, D.; Kudernac, T.; Puzys, A.; Feringa, B. L.; van Wees, B. J. *Adv. Mater.* **2007**, *19*, 2898−2902.
(18) Kiraly, P.; Soos, T.; Varga, S.; Vakulya, B.; Tarkanyi, G. *Magn. Reson. Chem.* **2010**, *48*, 13−19.
(19) Kusukawa, T.; Yoshizawa, M.; Fujita, M. *Angew. Chem., Int. Ed.* **2001**, *40*, 1879−1884.
(20) Lubbe, A. S.; Ruangsupapichat, N.; Caroli, G.; Feringa, B. L. *J. Org. Chem.* **2011**, *76*, 8599−8610.
(21) ter Wiel, M. K. J.; Feringa, B. L. *Tetrahedron* **2009**, *65*, 4332−4339.
(22) Schoevaars, A. M.; Kruizinga, W.; Zijlstra, R. W. J.; Veldman, N.; Spek, A. L.; Feringa, B. L. *J. Org. Chem.* **1997**, *62*, 4943−4948.
(23) Cross, W.; Hawkes, G. E.; Kroemer, R. T; Liedl, K. R.; Loerting, T.; Nasser, R.; Pritchard, R. G.; Steele, M.; Watkinson, M.; Whiting, A. *J. Chem. Soc., Perkin Trans. 2* **2001**, 459−467.
(24) Walko, M.; Feringa, B. L. *Chem. Commun.* **2007**, 1745−1747.
(25) Uchida, K.; Nakayama, Y.; Irie, M. *Bull. Chem. Soc. Jpn.* **1990**, *63*, 1311−1315.
(26) Irie, M.; Sakemura, K.; Okinaka, M.; Uchida, K. *J. Org. Chem.* **1995**, *60*, 8305−8309.
(27) Uchida, K.; Tsuchida, E.; Aoi, Y.; Nakamura, S.; Irie, M. *Chem. Lett.* **1999**, *28*, 63−64.
(28) Perrin, C.; Dwyer, T. *Chem. Rev.* **1990**, *90*, 935−967.
(29) Irie, M.; Lifka, T.; Uchida, K.; Kobatake, S.; Shindo, Y. *Chem. Commun.* **1999**, 747−750.
(30) Higashiguchi, H.; Matsuda, K.; Kobatake, S.; Yamada, T.; Kawai, T.; Irie, M. *Bull. Chem. Soc. Jpn.* **2000**, *73*, 2389−2394.
(31) Higashiguchi, H.; Matsuda, K.; Yamada, T.; Kawai, T.; Irie, M. *Chem. Lett.* **2000**, *29*, 1358−1359.
(32) Kitagawa, D.; Kobatake, S. *Chem. Lett.* **2011**, *40*, 93−95.